Biogeochemistry **69:** 125–141, 2004.

Characterization and origin of polar dissolved organic matter from the Great Salt Lake

JERRY A. LEENHEER[1,*], TED I. NOYES[1], COLLEEN E. ROSTAD[1] and M. LEE DAVISSON[2]

*[1]U.S. Geological Survey, P.O. Box 25046, MS 408, Bldg, 95, Denver Federal Center, Denver, Colorado 80225, USA; [2]Environmental Sciences Division, Lawrence Livermore National Laboratory, P.O. Box 808 L-231, Livermore, California 94550, USA; *Author for correspondence (e-mail: leenheer@usgs.gov)*

Received 24 April 2003; accepted in revised form 28 July 2003

Key words: Algae, Bacteria, Dissolved organic carbon, Dissolved organic matter, Salt water

Abstract. Polar dissolved organic matter (DOM) was isolated from a surface-water sample from the Great Salt Lake by separating it from colloidal organic matter by membrane dialysis, from less-polar DOM fractions by resin sorbents, and from inorganic salts by a combination of sodium cation exchange followed by precipitation of sodium salts by acetic acid during evaporative concentration. Polar DOM was the most abundant DOM fraction, accounting for 56% of the isolated DOM. Colloidal organic matter was ^{14}C-age dated to be about 100% modern carbon and all of the DOM fractions were ^{14}C-age dated to be between 94 and 95% modern carbon. Average structural models of each DOM fraction were derived that incorporated quantitative elemental and infrared, ^{13}C-NMR, and electrospray/mass spectrometric data. The polar DOM model consisted of open-chain *N*-acetyl hydroxy carboxylic acids likely derived from *N*-acetyl heteropolysaccharides that constituted the colloidal organic matter. The less polar DOM fraction models consisted of aliphatic alicyclic ring structures substituted with carboxyl, hydroxyl, ether, ester, and methyl groups. These ring structures had characteristics similar to terpenoid precursors. All DOM fractions in the Great Salt Lake are derived from algae and bacteria that dominate DOM inputs in this lake.

Introduction

Biogeochemical studies of dissolved organic matter (DOM) in salt waters are limited by the difficulty of DOM characterization when isolation of DOM from large amounts of salts is required. High molecular weight (HMW $>$ 1000 Da) DOM in salt waters can be isolated by tangential-flow ultrafiltration (Benner et al. 1992; Buesseler et al. 1996), but most marine dissolved organic carbon (DOC) (up to 70%) is low molecular weight (LMW) DOM (Amon and Benner 1996). Isolation of LMW DOM by sorption onto nonionic XAD-resins only recovers an additional 5–15% of the DOM (Benner et al. 1992), and this DOM is operationally classified as 'hydrophobic'. Therefore, the majority of marine DOM is polar LMW material and has never been isolated from salts. Another difficulty is the low concentration of marine DOM, especially in the deep ocean where DOC values average 45 μM (0.54 mgC/L) (Carlson and Ducklow 1995). These low DOM concentrations and large ratios of salt:DOM require isolation methods that can accommodate large volumes of water, high efficiencies of DOM separation from salt, and low DOM processing blanks.

A comprehensive approach for DOM fractionation and isolation was recently developed (Leenheer et al. 2000) that combined vacuum evaporation with dialysis to isolate HMW DOM, XAD resin sorption to isolate LMW hydrophobic DOM, and selective salt precipitations combined with vacuum evaporations to isolate LMW polar DOM. This DOM isolation method has been applied to fresh surface waters (Leenheer et al. 2000), and wastewater effluents and groundwaters (Leenheer et al. 2001a). The success of the method with wastewater effluents and groundwaters that had moderately large salt concentrations suggested application to natural salt water.

The Great Salt Lake was selected for the first application of this new isolation method because its reported DOC concentration ($\sim$20 mgC/L at the surface) is much greater than marine DOC and the organic geochemical processes that produce DOC have been investigated (Domalgalski et al. 1989). The salinity of the Great Salt Lake at the surface is 3–5 times the salinity of the ocean, but the salt composition is similar to marine salts (Domalgalski et al. 1989). The objectives of this report are to report on the efficiency of the DOM isolation method; to characterize isolated DOM by elemental, spectral and mass spectrometric techniques; and to relate these characterizations to DOM diagenesis.

Materials and methods

Sampling

Two 20-liter polyethylene carboys were filled with water sampled on 1 April, 2002 at the lake surface in the south arm of the Great Salt Lake at latitude 40°53′56″N, longitude 112°20′56″W. This sampling occurred before the annual green algae bloom that is responsible for the majority of annual productivity (Stephens and Gillespie 1976). The samples were shipped to the US Geological Survey National Water Quality Laboratory in Denver, CO where they were filtered through 25 and 1 µm glass fiber cartridge filters in series. Two subsamples (1 L and 100 mL) of filtered water were taken for DOC analyses.

DOM fractionation and isolation

A flow chart of the DOM fractionation and isolation procedure is shown in Figure 1. A number of changes were made in the comprehensive DOM isolation method (Leenheer et al. 2000) to accommodate the differences in salt water chemistry from fresh water chemistry. Firstly, the large salt concentration limits the utility of ion-exchange separations until the salts are reduced or removed. Therefore, the initial water-softening step by sodium exchange resin of the published method was eliminated, and the hydrophobic, transphilic, and colloid DOM fractions were isolated before inorganic salts were removed. Secondly, natural salt waters usually have much larger ratios of magnesium to sodium cations than fresh waters (Hem

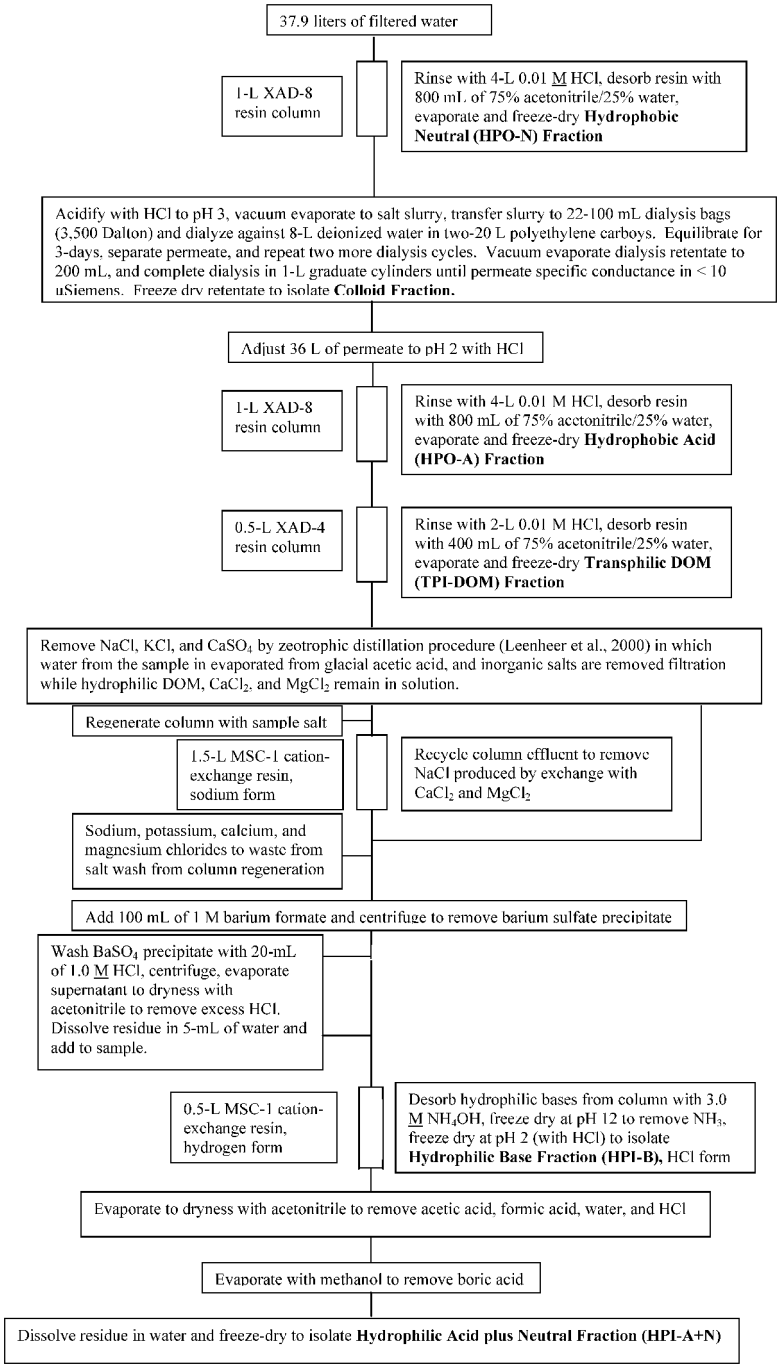

Figure 1. Comprehensive DOM fractionation and isolation flow chart for salt water.

1970). Magnesium chloride ion pair is soluble in acetic acid used to remove sodium chloride, potassium chloride, and calcium sulfate ion pairs (Audrieth and Kleinberg 1953). Therefore, the salt removal step by zeotrophic distillation with acetic acid was coupled with the water softening step to covert magnesium salts to sodium salts, and these two steps were repeated with sample salts used for resin regeneration to minimize the cation-exchange column size requirement. Lastly, the lack or low concentrations of silica, nitrate, and phosphate in the seawater sample allowed the elimination of steps to remove these constituents.

Spectral characterizations of DOM fractions

Infrared spectra were collected using 2–5 mg of DOM fraction isolates in KBr pellets. The Perkin Elmer System 2000 FT-IR used an infrared source with a pulsed laser carrier and a deuterated triglycine sulfate detector. The instrument was set up to scan from 4000 to 400 cm^{-1} averaging 10 scans at 1.0 cm^{-1} intervals with a resolution of 4.0 cm^{-1}. All spectra were normalized after acquisition to a maximum absorbance of 1.0 for comparative purposes.

CPMAS ^{13}C-NMR spectra were obtained on 20–200 mg of isolated DOM fractions. Freeze-dried samples were packed in zirconia rotors. CPMAS ^{13}C-NMR spectra were obtained on a 200-megahertz (MHz) Chemagnetics CMX spectrometer with a 7.5-mm-diameter probe. The spinning rate was 5000 Hz. The acquisition parameters included a contact time of 5 ms, pulse delay of 1 s, and a pulse width of 4.5 μs for the 90° pulse. Variable contact time studies by Alemany et al. (1983) indicate these are the optimum parameters for quantitatively determining different carbon structural group contributions to the NOM NMR spectra.

Electrospray/mass spectrometric characterization of the DOM fractions was conducted using a Hewlett Packard Series 1100 LC/MS with electrospray ionization. Samples were dissolved in UV grade 25/75 water/methanol at 5 mg/L and analyzed by flow injection analysis. The flow rate of the 25/75 water/methanol mobile phase was 0.2 mL/min. The quadrupole mass spectrometer scanned from 100 to 1000 m/z with capillary exit at 70 V for both positive and negative polarity. For electrospray ionization, the drying gas was 350 °C at 12 L/min with 35 psig nebulizer pressure, and capillary voltage of 4000 V. The scan range was often increased to 3000 to detect larger mass ions, along with ramped quadrupole voltages to increase high mass ion transmission. Source capillary exit voltage was decreased to 50 V, based on results with standards, to maximize formation of molecular ions and minimize adducts (positive mode) or fragmentations (negative mode). Although the instrument can scan down to m/z 50, the possibility of interference from solvent ions precluded this.

Organic carbon and elemental analyses

Huffman Laboratories, Golden, Colorado, conducted the subject analyses. DOC analysis was directly conducted on the 100 mL subsample by high temperature

combustion (ASTM Method D4129) with coulometric detection of CO_2 and indirectly conducted by measuring the percentage organic carbon in the salt (LECO CR-12 combustion) from freeze-drying 1-L of sample. Elemental analyses (C, H, O, N, S, Cl, and ash) of DOM fractions were conducted according to methods reported in Huffman and Stuber (1985).

Radiocarbon analytical method

Freeze-dried isolates were weighed and placed individually into 6 mm Vycor tubes, which were then inserted into 9 mm Vycor tubes along with a stoichiometric excess of CuO. The 9 mm tubes were evacuated, flamed sealed, and the isolates were combusted to CO_2 at 900 °C for 3 h in a muffle furnace. The CO_2 was cryogenically purified, converted into graphite at 570 °C in the presence of H_2 and a Fe catalyst (Vogel et al. 1987). The graphite was packed into an aluminum target, and analyzed for ^{14}C using an accelerator mass spectrometer at Lawrence Livermore National Laboratory. Raw data were corrected to recognized standards (Stuiver and Polach 1977) and converted to percent modern carbon (pmc). Combustion procedure blanks and reproducibility was 1 pmc. However, no ^{14}C procedural blanks or mass balance analysis were conducted during the comprehensive isolation procedures. Nevertheless, significant inclusion ($>1\%$) of organic solvents used during the isolation procedures and that potentially remained in the measured isolates was ruled out by their absence in spectral and LC/MS data. In addition, all isolation procedures that utilized organic solvents underwent freeze-drying steps in order to remove them.

Results

DOM fractionation and isolation

A bar diagram of DOM fractionation results is shown in Figure 2. The concentration of the colloid fraction underestimated actual concentrations because of losses that occurred when dialysis bag clamps on five of the 22 bags opened during the first dialysis cycle because of osmotic pressure. The hydrophilic acid plus neutral fraction concentration was also underestimated because of excessive recycling (seven cycles) required to remove calcium and magnesium by ion exchange after removal of sodium chloride by zeotrophic distillation with acetic acid. Only three softening cycles were theoretically required to convert calcium and magnesium salts to sodium chloride based upon proportions of these ions (Domagalski et al. 1989) and a present (2002) measured surface salinity of 14.5%. A tailing conductivity curve during deionized water rinses in the MSC-1 resin regeneration coupled with positive sulfate tests (barium sulfate precipitate) revealed that the porous resin beads were being fouled with a sulfate colloid (likely calcium sulfate). These colloidal sulfates were formed in the previous zeotrophic distillation step, and were not removed by filtration because of the

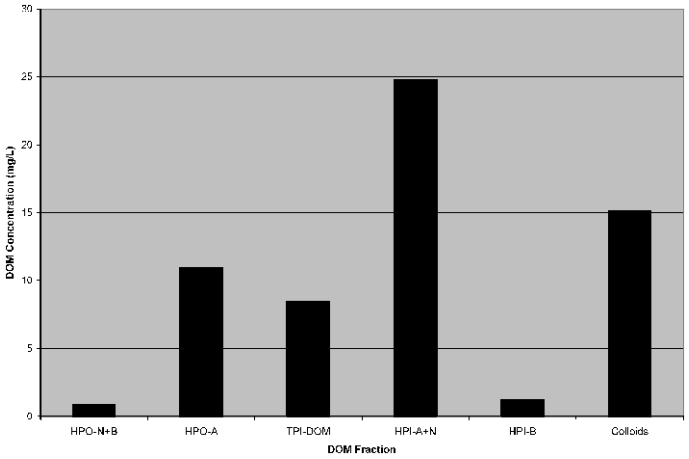

Figure 2. Bar diagram of DOM fractionation of Great Salt Lake. Fraction abbreviations are given in Figure 1.

Table 1. Elemental analyses and radiocarbon content of major DOM fractions from the Great Salt Lake (Results reported on a dried sample basis, NA = Not analyzed).

Fraction	%C	%H	%O	%N	%S	%Cl	%Ash	%Total	^{14}C (pmc)
Hydrophobic acid	54.52	5.88	34.33	2.02	NA	NA	2.80	99.55	94.6
Transphilic DOM	51.08	5.66	37.33	3.25	NA	NA	0.75	98.07	94.4
Hydrophilic acids plus neutrals	36.86	4.91	35.08	4.41	2.27	9.27	7.33	100.13	94.8
Colloids	40.78	5.67	41.91	3.62	NA	NA	10.28	102.26	104

coarse glass-wool filter used in the neck of the large funnel used to filter out salts. Extensive rinsing with deionized water restored resin capacity and enabled completion of the water-softening step in the procedure.

Organic carbon, elemental analyses, and radiocarbon content

DOC analyses by direct analyses of the water gave 40 and 41 mgC/L in duplicate determinations. Organic carbon percentages in the salt in 1 L of water were 0.046 and 0.051 in duplicate determinations. Based upon 116.1 g of salt weighed residue, these DOC determinations were computed to be 53 and 59 mgC/L.

Elemental analyses of the major DOM fractions are presented in Table 1. The sum of element percentage plus ash percentage is near 100% for all fractions that indicate quantitative accounting for the major elements. The significant chloride content for the hydrophilic acid plus neutral fraction is likely an artifact caused by HCl substitution with alcohols in this fraction during the final evaporation and drying steps of this fraction as shown in Figure 1.

Table 2. Radiocarbon of DIC in terrestrial rivers.

Sample	Latitude/longitude	Collection date	DIC (mg/L)	^{14}C (pmc)
San Carlos River, AZ	33°17′50″/110°27′02″	7/1/94	243	99
Gila River, AZ	33°09′54″/110°08′06″	7/1/94	322	106
Rio Grande River, NM	32°12′25″/106°45′33″	7/2/94	159	101
Red River, TX	33°36′28″/93°48′55″	7/4/94	164	108
Missouri River, MS	38°50′26″/90°14′10″	3/27/97	200	100
Missouri River, MS	38°50′26″/90°14′10″	7/23/97	–	109
Mississippi River, IL	38°59′49″/90°40′45″	3/27/97	231	85
Mississippi River, IL	38°59′49″/90°40′45″	7/23/97	193	101
Illinois River, IL	39°09′28″/90°36′49″	3/27/97	252	93
Illinois River, IL	39°09′28″/90°36′49″	11/3/97	235	117

The DOC recovery based upon fraction weights and elemental analyses is computed to be 24.9 mgC/L. Thus, percent DOC recoveries are 62% for a DOC of 40.5 mg/L or 44% for a DOC of 56 mg/L.

Radiocarbon contents of the DOM fractions are presented in Table 1. Radiocarbon contents of dissolved inorganic carbon (DIC) in various terrestrial rivers are presented in Table 2.

Infrared spectra of DOM fractions

Infrared spectra of DOM fractions are presented in Figure 3. A major peak in all DOM fractions is the 1720 cm^{-1} peak of carboxylic acids except for the colloid fraction. A peak at 1660 cm^{-1} indicative of amides (amide I band) is found in the hydrophobic neutral, hydrophilic acid plus neutral, hydrophilic base, and colloid fractions. An additional amide peak (amide II band) near 1550 cm^{-1}, which is specific for secondary amides, is found for the hydrophilic acid plus neutral and colloid fractions. The greater intensity of the amide I band compared to the amide II band, plus the broad N-H bending band from 500–700 cm^{-1} are two indicators for the presence of primary amides for the specified DOM fractions. Another indicator of primary amide structures is that ammonium chloride peaks were found in the infrared spectrum (spectrum not shown) of the hydrophilic acid plus neutral fraction after hydrolysis with HCl.

Alcohols are indicated in the hydrophobic neutral, hydrophilic acid plus neutral, and colloid fractions by broad peaks at 3300–3400 and 1000–1150 cm^{-1}. Aliphatic hydrocarbons in the hydrophobic fractions are indicated by peaks at 2960, 2930, 1460, and 1380 cm^{-1}. The base fraction has a broad N-H stretching band from 2800 to 3200 cm^{-1}. Peaks caused by inorganic borate, carbonates, phosphates, silicates, and sulfates are absent in all spectra.

^{13}C-NMR spectra of DOM fractions

^{13}C-NMR spectra of DOM fractions are presented in Figure 4. Aliphatic C-H, C-C, and C-N carbon linkages occur from 0 to 60 ppm; aliphatic C-O linkages (alcohols, esters,

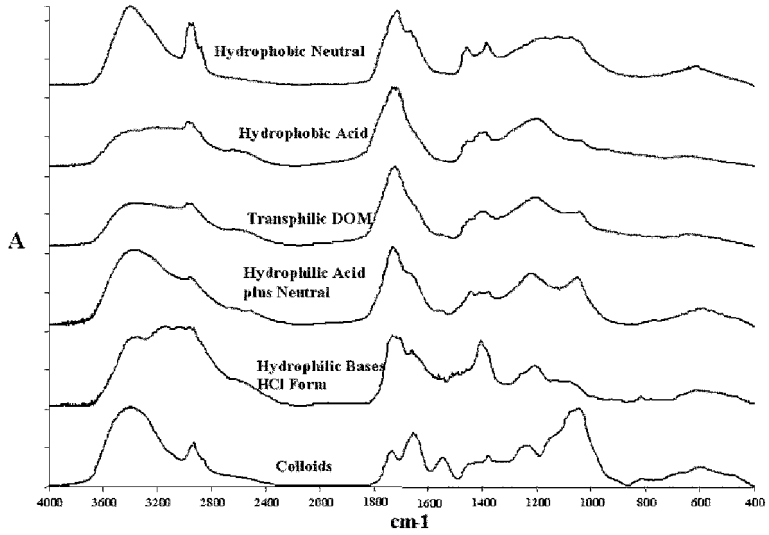

Figure 3. Infrared spectra of DOM fractions from the Great Salt Lake.

and ethers) occur from 60 to 90 ppm, anomeric carbon linkages of carbohydrates (O-C-O) occur from 90 to 110 ppm; aromatic and olefinic carbon linkages occur from 110 to 160 ppm; carbonyl groups of amides, carboxylic acids, and esters occur from 160 to 190 ppm; and carbonyl groups of ketones occur from 190 to 220 ppm. The number of carbons in an empirical formula calculated from the elemental analyses apportioned to each structural region of the ^{13}C-NMR spectra is shown in Table 3 for the hydrophobic acid, transphilic NOM, hydrophilic acids plus neutrals, and colloid fractions. For the aliphatic hydrocarbon region from 0 to 60 ppm for the hydrophobic acid and transphilic NOM fractions, the peak near 20 ppm is caused by methyl groups and a portion of the peak near 45 ppm is caused by quaternary aliphatic carbon based upon dipolar dephased ^{13}C-NMR spectra which detects only methyl and quaternary carbon groups (dipolar-dephased ^{13}C-NMR spectra not shown). The remainder of the 45 ppm peak is caused by methine carbons on alicyclic rings as indicated by ring content analyses in Table 3. Methylene groups indicative of straight chain hydrocarbons are only significant for the hydrophobic neutral fraction.

The peak at 52 ppm for the hydrophilic acid plus neutral fractions is also a methyl group and its chemical shift is indicative of a methyl ester. This was confirmed by subjecting a portion of this fraction to hydrolysis in 1.0 M HCl at 100 °C for 1 h followed by vacuum evaporation of the reagents. After hydrolysis, methyl peak near 52 disappeared in the ^{13}C-NMR spectrum (spectrum not shown), but the methyl peak at 20 ppm remained. It is likely that methyl esters were created in this fraction by esterification reactions with the methanol used to remove boric acid during the isolation of this fraction.

The hydrophobic hydrocarbon structures (aliphatic hydrocarbon and aromatic hydrocarbons) decreased in the order HPO-N > HPO-A > TPI-NOM > HPI-

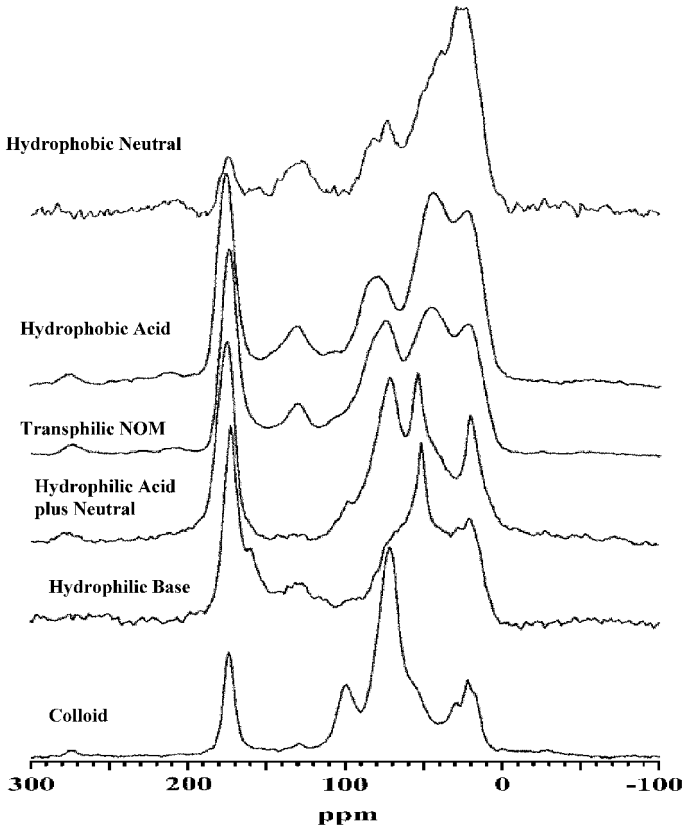

Figure 4. ^{13}C-NMR spectra of DOM fractions from the Great Salt Lake.

A + N = HPI-B = colloids, and the polar structures (carboxyl, amide, amines, and alcohols) increased in the fractions in the same order. The peak at 52 ppm for the hydrophilic base fractions is caused by C-N linkages of amines or amides; this peak cannot be a methyl ester as methyl esters are not indicated by the infrared spectrum of this fraction shown in Figure 3. The only fraction with significant carbohydrate content is the colloid fraction as indicated by the anomeric carbon peak near 105 ppm for this fraction. Aromatic carbon contents are lower than found for corresponding DOM fractions isolated from terrestrial waters with allochtonous inputs of tannins and lignins, and peaks (140–160 and 110–120 ppm) caused by phenol structures in tannins and lignins are not significant in the spectra.

Electrospray/mass spectrometry

Electrospray/mass spectra of selected DOM fractions are presented in Figure 5. The spectra of these fractions indicate that the molecular-weights of these fractions are relatively small and the molecular mixture complexity is great with the qualification

Table 3. Data used to determine structural characteristics of DOM fractions.

Determination	Method	Hydrophobic acids	Transphilic DOM	Hydrophilic acids + neutrals	Colloids
Empirical formula (1000 Da) (Normalized to C_{40})	Elemental analyses	$C_{46.7}H_{60.5}O_{22}N_{1.5}$ $C_{40}H_{51.8}O_{18.9}N_{1.3}$	$C_{42.9}$ $H_{57}O_{23.5}N_{2.3}$ $C_{40}H_{53.1}O_{21.9}N_{2.1}$	$C_{33.3}H_{53.3}O_{23.8}N_{3.4}S_{0.8}Cl_{2.8}$ $C_{40}H_{64}O_{28.6}N_{4.1}S_1Cl_{3.4}$	$C_{37.9}H_{63.2}O_{29.2}N_{2.9}$ $C_{40}H_{66.7}O_{30.8}N_{3.1}$
Aliphatic C–H plus C–N carbons	%C from ^{13}C-NMR times #C's in 1000 Da formula	23.2	19.2	13.4	9.4
Aliphatic C–O carbons	%C from ^{13}C-NMR times #C's in 1000 Da formula	8.2	10.2	9.4	19.1
Anomeric O–C–O carbons	%C from ^{13}C-NMR times #C's in 1000 Da formula	1.1	1.1	1.7	4.5
Aromatic plus olefinic carbons	%C from ^{13}C-NMR times #C's in 1000 Da formula	4.5	3.2	1.4	0.4
Carbonyl C=O carbons	%C from ^{13}C-NMR times #C's in 1000 Da formula	9.8	9.3	7.4	4.5
Index of Hydrogen deficiency (Φ)	$\Phi = [(2C + 2) - (H + Cl - N)]/2$	18.2	16.6	8.0	8.8
# Rings (θ)	$\theta = \Phi - C = O\ C - 0.5$ (aromatic plus olefinic C)	6.2	5.7	−0.1	4.1
# C per ring (Ω)	Ω = Total C/θ	7.5	7.5	No rings	9.2

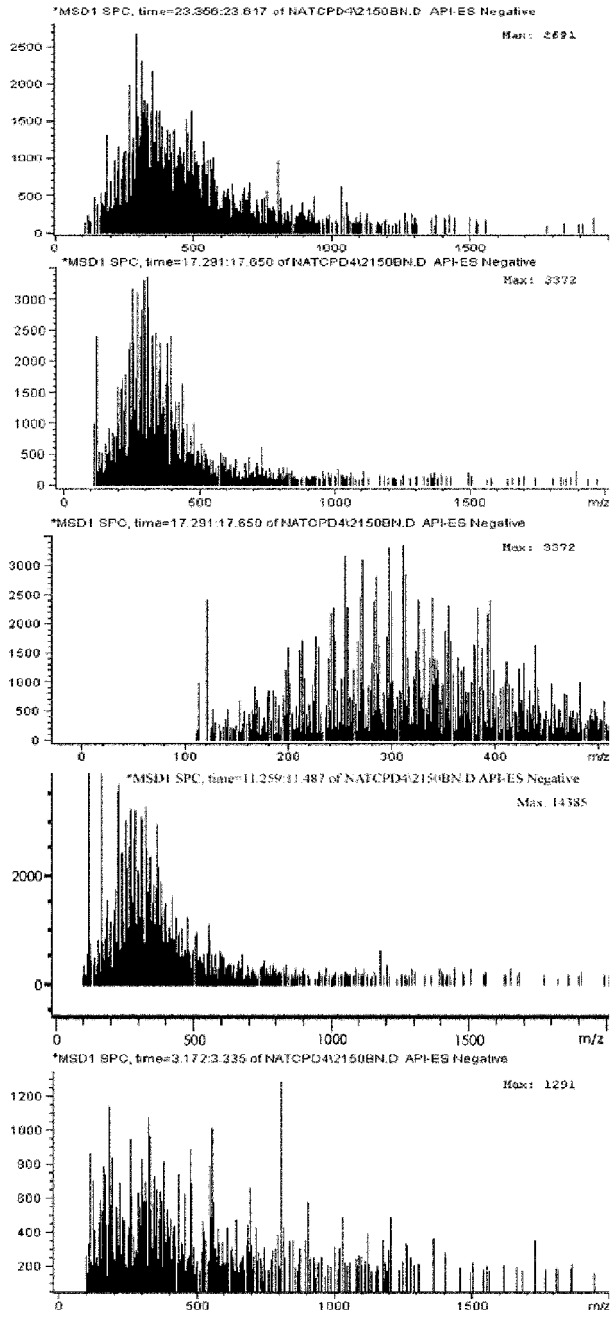

Figure 5. Electrospray ionization, negative ion mass spectra of selected DOM fractions from the Great Salt Lake. Fraction abbreviations are given in Figure 1.

that multiply charged ions and molecular aggregates and adducts can affect both molecular weight distributions and mixture complexity. There are no ions indicative of aromatic sulfonates and alkylphenol polyethoxylate carboxylates that are metabolites of surfactants commonly found in water.

The hydrophobic neutral, hydrophobic acid, and transphilic NOM fractions had clusters of ions differing by 14 m/z which is indicative of methylene group differences caused by variable aliphatic chain lengths, alicyclic ring sizes, and/or methyl group contents. It was difficult to obtain reproducible spectra for the hydrophilic acid plus neutral fraction. Tailing of the total ion current infusion curve indicated interactions with the components of the mass spectrometer. The spectrum of this fraction (Figure 5) was weak in ion intensity and clusters of ions occurred out to about 1300 m/z which may indicate the presence of molecular aggregates. The low molecular-weight ions (<300 m/z) of the hydrophilic acid plus neutral spectrum, where molecular aggregates are not likely, had predominately odd masses that is indicative of structures containing either no or two nitrogens per molecule.

Discussion

DOM fractionation and isolation

The fractionation and isolation procedure of Figure 1 could be improved by some simple changes to increase DOM recoveries. Firstly, recoveries of the colloid fraction could be increased by double clamping the dialysis bags to prevent clamp opening because of osmotic pressure. Secondly, supercentrifugation should be combined with filtration to remove sulfate colloids after the zeotrophic distillation steps of Figure 1 to remove salts. Removal of these sulfate colloids will prevent resin fouling during the sodium softening steps. Lastly, the final drying steps of the hydrophilic acid plus neutral fraction to remove boric acid and HCl could be performed under higher vacuums and lower temperatures to minimize addition of methyl groups and chloride to this fraction. These improvements are needed to isolate polar DOM fractions from marine waters where the ratio of DOM to salt is lower than in the Great Salt Lake. The low DOM concentration of marine waters is not an intractable limitation as DOM in groundwaters with similar DOM concentrations were fractionated and characterized by ^{13}C-NMR and IR spectrometry on 100 L of sample (Leenheer et al. 2001b). If greater amounts of DOM fraction isolates are required for additional analyses, the sample size can be increased to 1000 L and be preconcentrated by a combination of reverse osmosis and vacuum evaporation before DOM fractionation (AWWARF 2001).

Radiocarbon content of GSL DOM fractions

The ^{14}C content of DOM isolates in the GSL was essentially bimodal, with the colloidal fraction measured at 104 pmc and the HPO, TPI, and HPI fractions all approximately 95 pmc. Although data is not extensive, the ^{14}C content of terrestrial

river and lake derived DOM ranges from about 85 to 120 pmc (Hedges et al. 1986; Raymond and Bauer 2001; Davisson 2002). In marine systems, DOM ranges from around 50 pmc to modern, with the highest content being associated with HMW material in near-surface environments (Williams and Druffle 1987; Druffel and Williams 1990; Santschi et al. 1995). Open ocean ^{14}C measurements of DOM represent relative ages of autotrophic-derived material, whose carbon source is ultimately derived from DIC in the photic zone and is in approximate isotopic equilibrium with the atmosphere.

Assuming that terrestrial DOM input in the GSL is small relative to primary production by algae (Stephens and Gillespie 1976) and is removed by photolytic oxidation, then the ^{14}C reflects the relative age distribution among the DOM fractions in this autotrophic driven system. Chemical and spectroscopic evidence presented thus far demonstrates the structural similarities of the colloidal fraction (analogous to marine HMW fraction) to bacterial cell wall components (i.e., *N*-acetyl polysaccharides). However, its ^{14}C content is approximately 6 pmc lower than the content in modern atmospheric CO_2 (assumed to be 110 pmc in the GSL vicinity). This suggests that the autotrophic bacteria generating colloidal material fixes DIC from a source with a ^{14}C content less than modern (GSL $DI^{14}C$ not measured in this study). A similar effect was observed for some lakes in the McMurdo Dry Valleys of Antarctica where DIC fixed by autotrophs was derived from relict CO_2 in glacial melt (Doran et al. 1999). Furthermore, as shown in Table 3, the ^{14}C content of many major rivers in the continental US are lower than atmospheric CO_2 levels, owing to contributions from older terrestrially derived inorganic carbon sources (Davisson 2002). It is therefore likely that the colloidal fraction of DOM in the GSL is essentially modern and the bacterial consortium it represents fixed carbon from DIC with a ^{14}C content of 104 pmc. Consequently, if the HPO, TPI, and HPI fractions (representing LMW DOM) are derived from decay of the same bacterial consortium, then their ^{14}C content indicates an older age than that of its parent material.

The ^{14}C content of these three factions can be taken at face value to calculate an age. In this case, the 95 pmc would suggest a mean age of approximately 400 years using a 5730 year half-life for ^{14}C. However, this age ignores the contribution from bomb-pulse ^{14}C and the isotopic dis-equilibrium between DIC and atmospheric CO_2. Therefore, it is more accurate to assume that the HPO, TPI, and HPI fractions measured in this study were derived from a pre-bomb carbon source (ca. mid-1950s). Given the indirect evidence that the ^{14}C of the DIC pool in the GSL is less than atmospheric CO_2 by approximately 6 pmc, then the ^{14}C content in these three fractions would essentially be the same as a pre-bomb DIC pool in the GSL (i.e., 94 pmc) when the ^{14}C of atmospheric CO_2 was 100 pmc. Consequently, the mean age of the HPO, TPI, and HPI fractions could be as young as approximately 45 years, corresponding to the period just before ^{14}C levels began to increase.

Average structural models of DOM fractions

The elemental and spectral data can be combined to form average molecular structures for the four major DOM fractions. These structures are shown in Figure

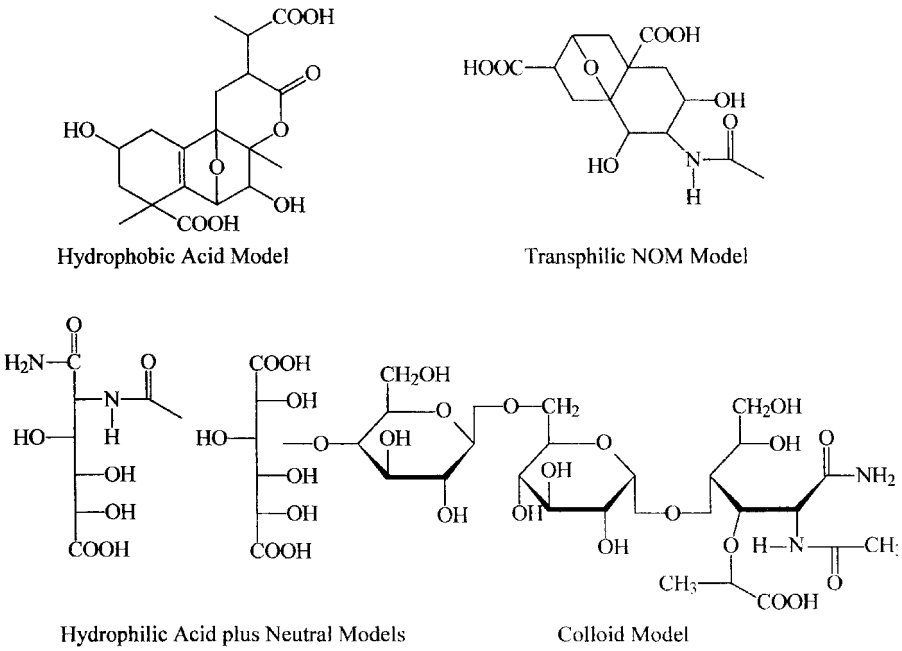

Figure 6. Average structural models of NOM fractions from the Great Salt Lake.

6. These models should not be perceived as actual structures, but are useful for imaging the compound-class characteristics of each fraction. Each model was constructed to fit the empirical formula and structural functional group data of Table 3. The hydrophobic acid model of Figure 6 is a complex ring structure with branched methyl groups and quaternary carbon linkages. This structure is clearly representative as being derived from terpenoid hydrocarbon precursors. Primary production of algae and secondary production of bacteria in the Great Salt Lake is the likely source of terpenoid precursors as pigments and steroids. The model of Figure 6 indicates extensive oxidative degradation of these terpenoid precursors by the presence of carboxyl and hydroxyl groups, and by the absence of double bonds and straight-chain hydrocarbon structures that are easily oxidized.

The transphilic NOM model also has a complex ring structure that is indicative of terpenoid precursors. The *N*-acetyl functional group probably does not belong attached to the model structure as shown, but it probably belongs to compound class represented by the hydrophilic acid plus neutral model. As the name indicates, the transphilic NOM fraction has intermediate polarity between the hydrophobic and hydrophilic fractions, and both types of molecules are found in this fraction.

The hydrophilic acid plus neutral fraction compound-class structure is of greatest interest based upon the objectives of this report. The empirical formula used in the construction of these two models was adjusted to remove the methyl esters and chloride groups (methyl esters were replaced with carboxyl groups and chloride groups were replaced this hydroxyl groups) that were artifacts of the isolation

procedure. The model is an oxidized amino sugar acid derived from amino sugar precursors such as chitin, bacterial cell-wall peptidoglycans, and glycoproteins. The evidence for the *N*-acetyl groups in this model is strong based upon the methyl of the *N*-acetyl groups of the ^{13}C-NMR spectra (20 ppm peak in Figure 4) that did not change when this fraction was hydrolyzed. Amides are much more resistant to acid hydrolysis than esters. The 1550 cm^{-1} amide II band of the infrared spectra (Figure 3) is also indicative of secondary amide *N*-acetyl groups. The primary amide structure (also found in the colloid model) is postulated to be derived from degradation of glycoproteins in which asparagine is linked to the carbohydrate (Lehninger et al. 1993) and is degraded as shown in the following reaction:

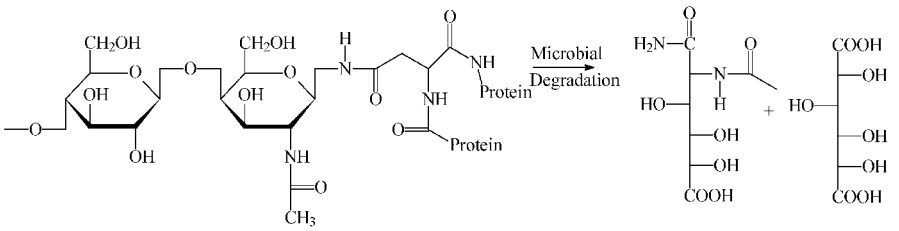

The complex molecular weight distribution of hydrophilic acid plus neutral fraction indicated by the electrospray/mass spectrum can be explained by varying degrees of molecular aggregation, varying degrees of carboxyl group methylation, varying degrees of oxidation of terminal carbons to carboxyl groups, and varying amounts of *N*-acetyl substituents. The ring content data (0 rings) of Table 4 is indicative of carbohydrate ring opening as contrasted with the rings in the colloid model. Open-chain sugar acids form lactone rings in the acid form, and it is likely that methanol treatment in the presence of HCl during the isolation steps resulted in transesterification/methylation that opened up the lactone rings.

The colloid model is presented as a *N*-acetyl heteropolysaccharide. The ^{13}C-NMR spectra of this colloid fraction is nearly identical to spectra for HMW DOM isolated from fresh waters and marine waters by Repeta et al. (2002). The monosaccharide composition is likely composed of rhamnose, fucose, arabinose, xylose, mannose, glactose, glucose, glucosamine, galactosamine, glucuronic acid, and galacturonic acid as was found for several HMW DOM isolates from fresh waters and marine waters by Repeta et al. (2002). The average model data clearly indicates that only one ring in two has *N*-acetyl groups. The spectral data also does not show any evidence for peptide structures that might be expected for peptidoglycans, but the small peak near 18 ppm (Figure 4) might be indicative of a methyl group of a bound lactic acid side chain found in muramic acid constituents of peptidoglycans, or it might be the methyl group in rhamnose. The carboxylic acid group of this model is seen in the acid form in the infrared spectra of Figure 3 by the peak near 1720 cm^{-1}. The primary amide structure was derived as shown previously for the hydrophilic acid plus neutral fraction. The molecular weight of this colloid is greater than 3500 Da of the dialysis membrane used in its isolation.

Acknowledgements

We thank David V. Allen of the Utah District Office, US Geological Survey, for the collection and shipment of the Great Salt Lake sample. Use of trade names in this report is for identification purposes only and does not constitute endorsement by the US Geological Survey.

References

Alemany L.B., Grant D.M., Pugmire R.J., Alger T.D. and Zilm K.W. 1983. Cross polarization and magic angle sample spinning NMR spectra of model organic compounds: 2. Molecules of low or remote protonation. J. Am. Chem. Soc. 105: 2142–2147.

AWWARF, American Water Works Association Research Foundation 2001. Polar NOM: Characterization, DBP's, Treatment. AWWARF, Denver, CO, pp. 3-1–3-26.

Amon M.W.R. and Benner R. 1996. Bacterial utilization of different size classes of dissolved organic matter. Limnol. Oceanogr. 4: 41–51.

Audrieth L.F. and Kleinberg J. 1953. Non-Aqueous Solvents: Applications as Media for Chemical Reactions, Chapter 8, Acetic Acid. John Wiley and Sons, New York, pp. 148–151.

Benner R., Pakulski J.D., McCarthy M., Hedges J.I. and Hatcher P.G. 1992. Bulk chemical characteristics of dissolved organic matter in the ocean. Science 225: 1561–1564.

Buesseler K.O., Bauer J.E., Chen R.F., Eglinton T.I., Gustafsson O., Landing W., Mopper K., Moran S.B., Santschi P.H., VernonClark R. and Wells M.L. 1996. An intercomparison of cross-flow filtration techniques used for sampling marine colloids: overview and organic carbon results. Mar. Chem. 55: 1–31.

Carlson C.A. and Ducklow H.W. 1995. Dissolved organic carbon in the upper ocean of the central equatorial Pacific Ocean, 1992: daily and fine scale vertical variations. Deep-Sea Res. 42: 639–656.

Davisson M.L. 2002. Isotopic Tracers in Surface Water. American Water Works Association Research Foundation, Denver, CO.

Domagalski J.L., Orem W.H. and Eugster H.P. 1989. Organic geochemistry and brine composition in Great Salt, Mono, and Walker Lakes. Geochim. Cosmochim. Acta 53: 2857–2872.

Doran P.T., Berger G.W., Lyons W.B., Wharton R.A., Davisson M.L., Southon J. and Dibb J.E. 1999. Dating Quaternary lacustrine sediments in the McMurdo Dry Valleys, Antarctica. Paleogeo. Paleoclim. Paleoecol., 147: 223–239.

Druffle E.R.M. and Williams P.M. 1990. Identification of a deep marine source of particulate organic carbon using bomb ^{14}C. Nature 347: 172–174.

Hedges J.I., Ertel J.R., Quay P.D., Grootes P.M., Richey J.E., Devol A.H., Farwell G.W., Schmide F.H. and Salati E. 1986. Organic carbon-14 in the Amazon River system. Science 231: 1129–1131.

Hem J.D. 1970. Study and Interpretation of the Chemical Characteristics of Natural Water. U.S. Geological Survey Water-Supply Paper 1473. 2nd ed., US Geological Survey, Washington, DC.

Huffman Jr. E.W.D. and Stuber H.A. 1985. Analytical methodology for elemental analyses of humic substances. In: Aiken G.R., McKnight D.M., Wershaw R.L. and MacCarthy P. (eds) Humic Substances in Soil, Sediment, and Water: Geochemistry, Isolation, and Characterization. John Wiley and Sons, New York,pp. 433–455.

Leenheer J.A., Croue J.-P., Benjamin M., Korshin G.V., Hwang C.J., Bruchet A. and Aiken G. 2000. Comprehensive isolation of natural organic matter for spectral characterization and reactivity testing. In: Barrett S., Krasner S.W. and Amy G.L. (eds) Natural Organic Matter and Disinfection By-Products. American Chemical Society Symposium Series 761. American Chemical Society, Washington, D.C.,pp. 68–83.

Leenheer J.A., Hsu J. and Barber L.B. 2001. Transport and fate of organic wastes in groundwater at the Stringfellow hazardous waste disposal site, southern California. J. Contam. Hydrol. 51: 163–178.

Leenheer J.A., Rostad C.E., Barber L.B., Schroeder R.A., Anders R. and Davisson M. 2001. Nature and chlorine reactivity of organic constitutents from reclaimed water in groundwater, Los Angeles County, California. Environ. Sci. Technol. 35: 3869–3876.

Lehninger A.L., Nelson D.L. and Cox M.M. 1993. Principles of Biochemistry. 2nd edn. Worth Publishers, New York, pp. 315–318.

Raymond P.A. and Bauer J.E. 2001. Use of ^{14}C and ^{13}C natural abundances for evaluating riverine, estuarine, and coastal DOC and POC sources and cycling: a review and synthesis. Org. Geochem. 32: 469–485.

Repeta D.J., Quan T.M., Aluwihare L.I. and Accardi A.M. 2002. Chemical characterization of high molecular weight dissolved organic matter in fresh and marine waters. Geochim. Cosmochim. Acta 66: 955–962.

Santschi P.H., Guo L., Baskaran M., Trumbore S., Southon J., Bianchi T.S., Honeyman B. and Cifuentes L. 1995. Isotopic evidence for the contemporary origin of high-molecular weight organic matter in oceanic environments. Geochim. Cosmochim. Acta 59: 625–631.

Stephens D.W. and Gillespie D.M. 1976. Phytoplankton production in the Great Salt Lake, Utah, and a laboratory study of algal response to enrichment. Limnol. Oceanogr. 21: 74–87.

Stuiver M. and Polach H. 1977. Reporting of ^{14}C data. Radiocarbon 19: 355–363.

Vogel J.S., Southon J.R. and Nelson D.E. 1987. Catalyst and binder effects in the use of filamentous graphite in AMS. Nucl. Instrum. Meth. Phys. Res. B29: 50–56.

Williams P.M. and Druffle E.R.M. 1987. Radiocarbon in dissolved organic matter in the central North Pacific Ocean. Nature 330: 246–248.